

Ultrastructure and Mechanics of Annealed *Nephila clavipes* Major

Ampullate Silk

Supporting Information

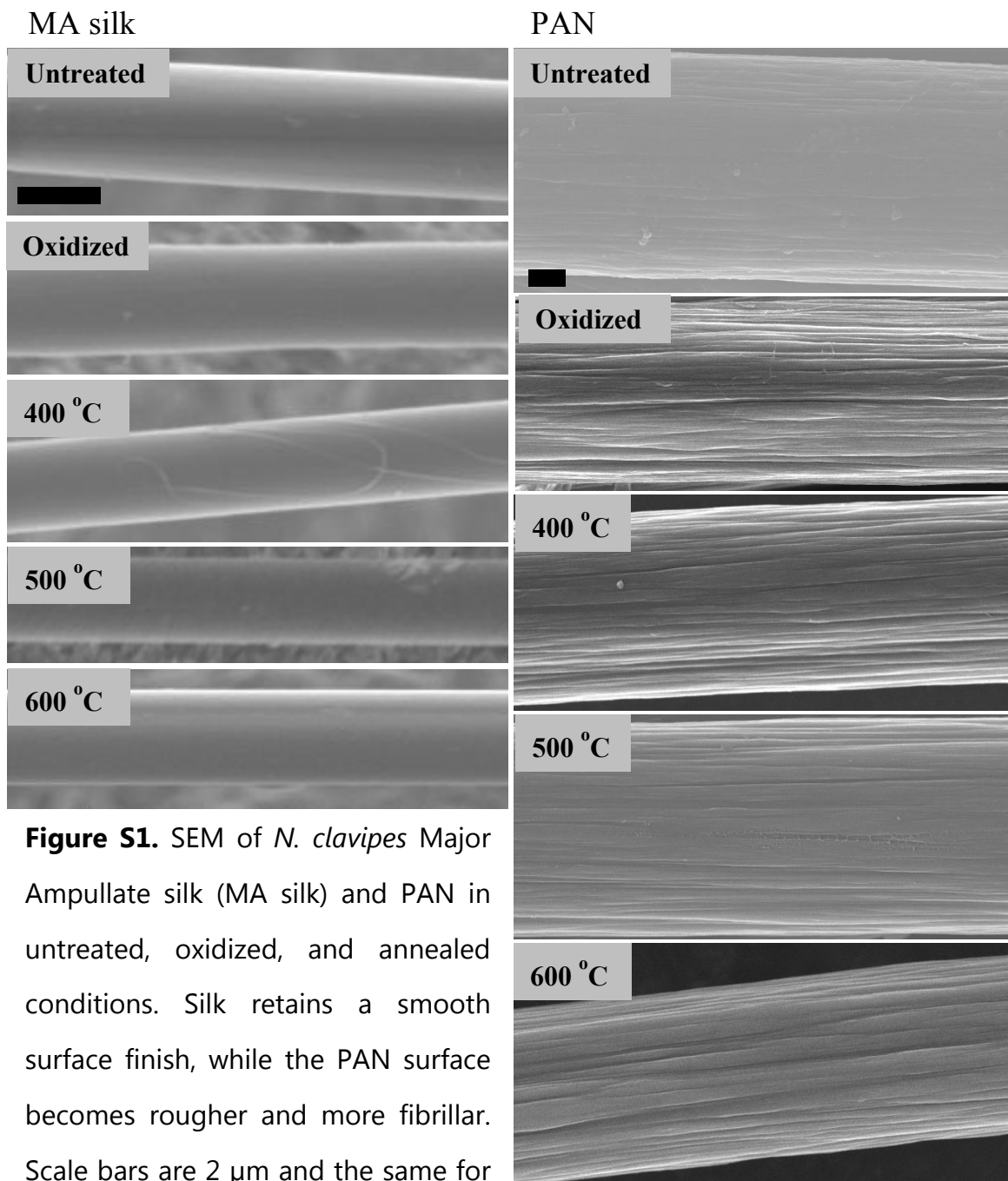


Figure S1. SEM of *N. clavipes* Major Ampullate silk (MA silk) and PAN in untreated, oxidized, and annealed conditions. Silk retains a smooth surface finish, while the PAN surface becomes rougher and more fibrillar. Scale bars are 2 μm and the same for the silks and PAN, respectively.

Although single fiber mechanical testing can show truer mechanical properties, without any contributions from fiber weaving or slip between fibers, it has inherent difficulties that can lead to sources of error. Fibers must be individually mounted for tensile testing by hand, which can result in fibers being slightly misaligned and not parallel to the loading direction. We analyzed each load-deflection curve individually and determined where initial loading began, defined as the point where the slope was constant and within 90% of the calculated Young's Modulus. All these factors, in addition to biological variation and processing defects, can explain the spread in the stress-strain plots.

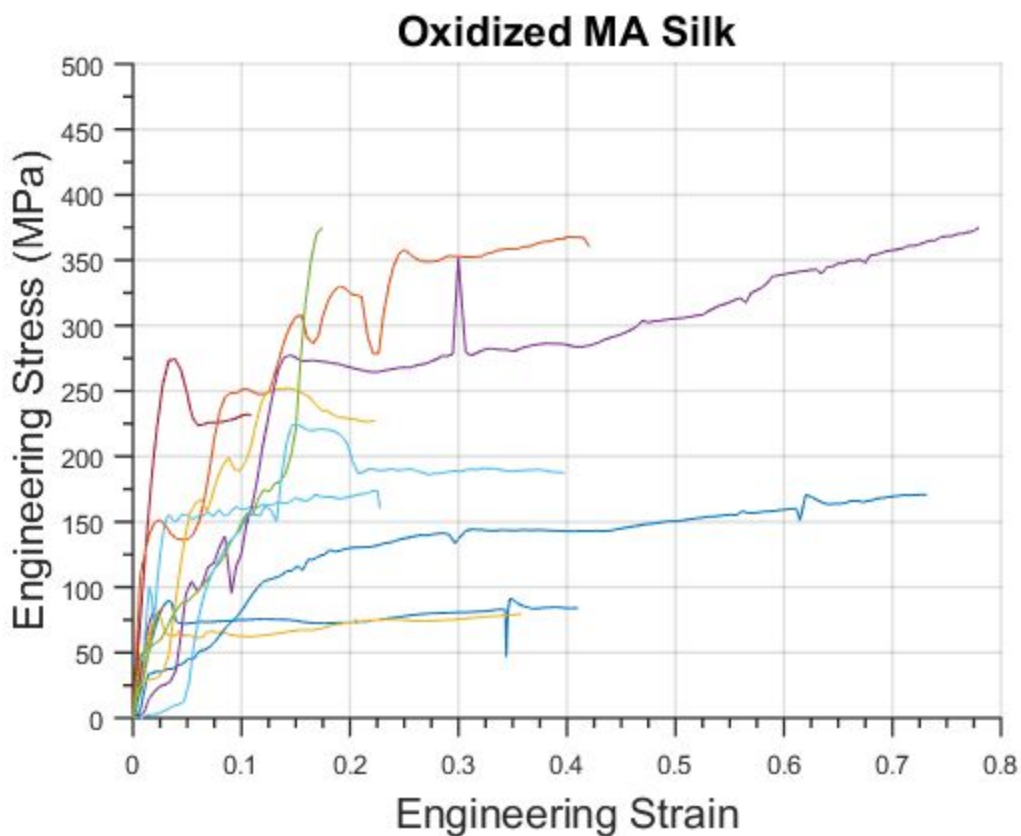


Figure S2. Stress-strain plots of 13 oxidized fibers tested showing a wide range of behaviors from elastomeric to brittle. This spread made the error in calculated stiffness and strength too high to report with confidence.

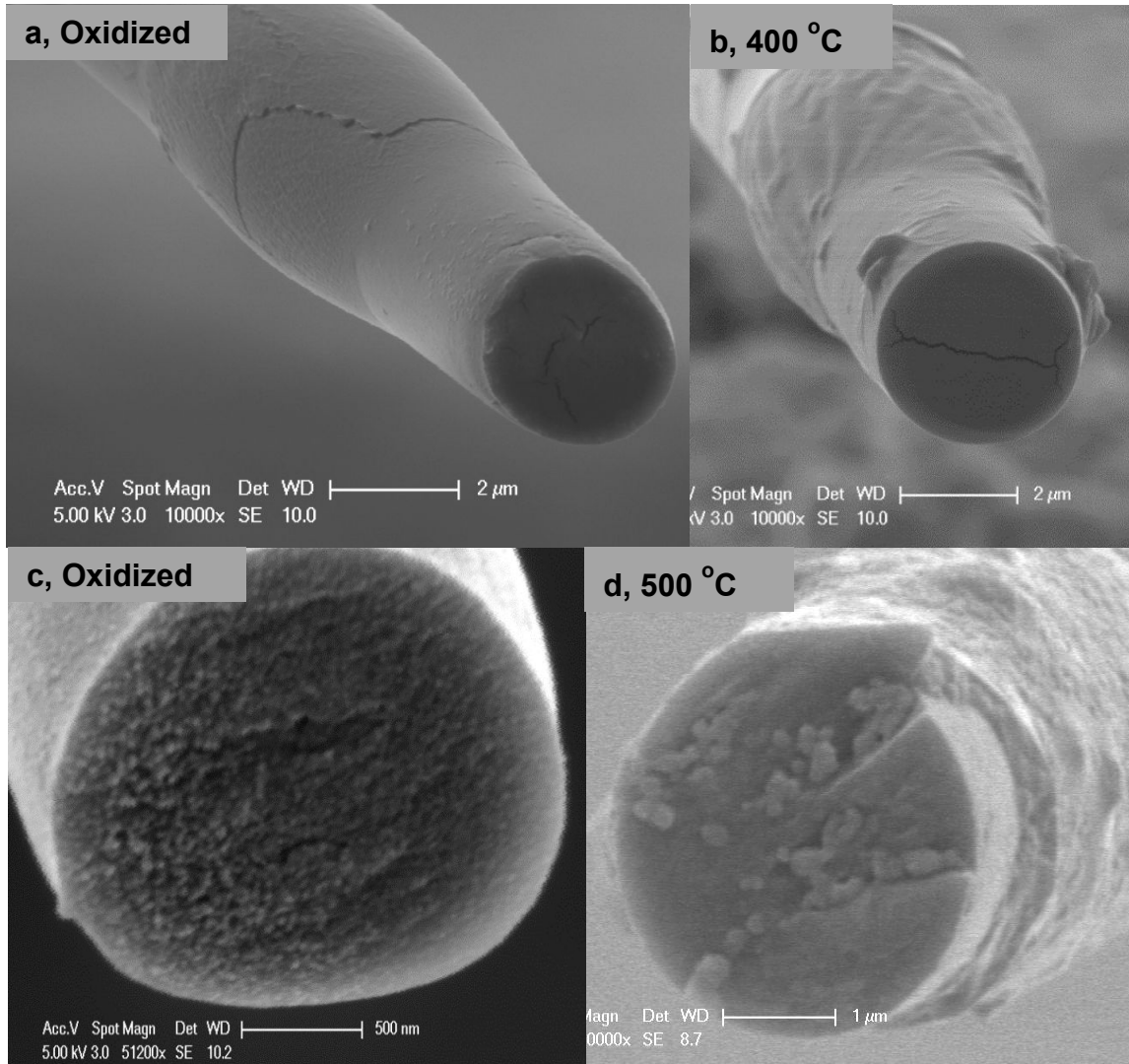


Figure S3. Additional MA silk fracture surfaces showing necking (a, b), possible nanofibrils where the spidroins have cyclized individually but not fused together (c), and core-shell structures (d), identified by contrast differences, crack deflection, or sword-in-sheath fracture.

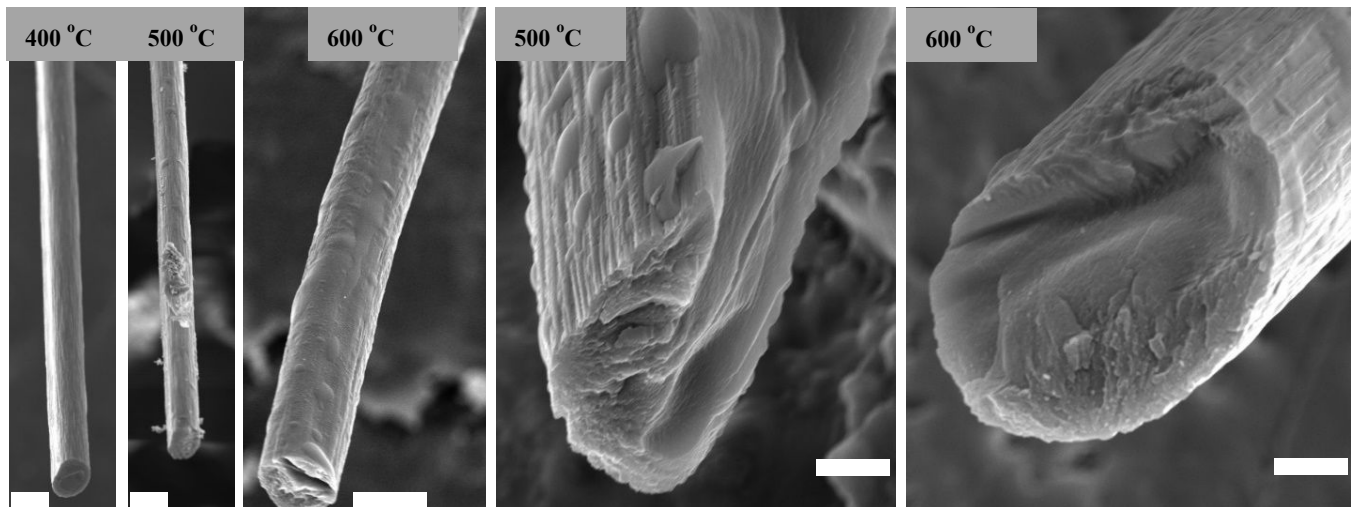


Figure S4. Fractured PAN fibers show no necking (left three micrographs, scale bars 10 microns). Some 500 and 600 °C fibers failed via shear across the entire fiber cross section (right two micrographs, scale bars 2 microns).

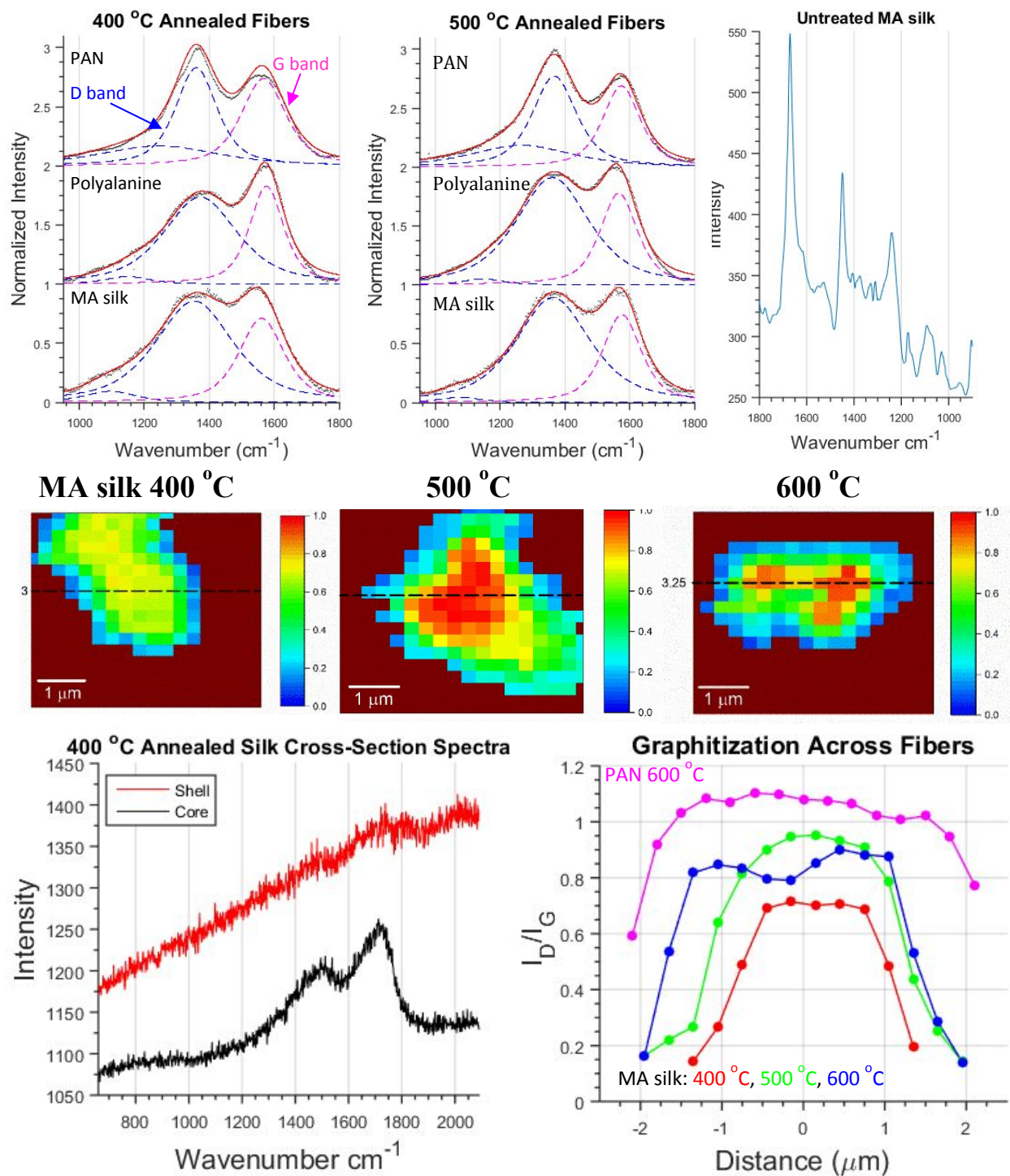


Figure S5. Deconvolution of Raman spectra from 400 °C and 500 °C MA silk also shows no significant difference in graphitization and the absence of the amide band from untreated fibers. Raman maps show a core-shell distribution if I_D/I_G ratios tending towards a more graphitic shell, but data from the shell has a very low signal to noise ratio.

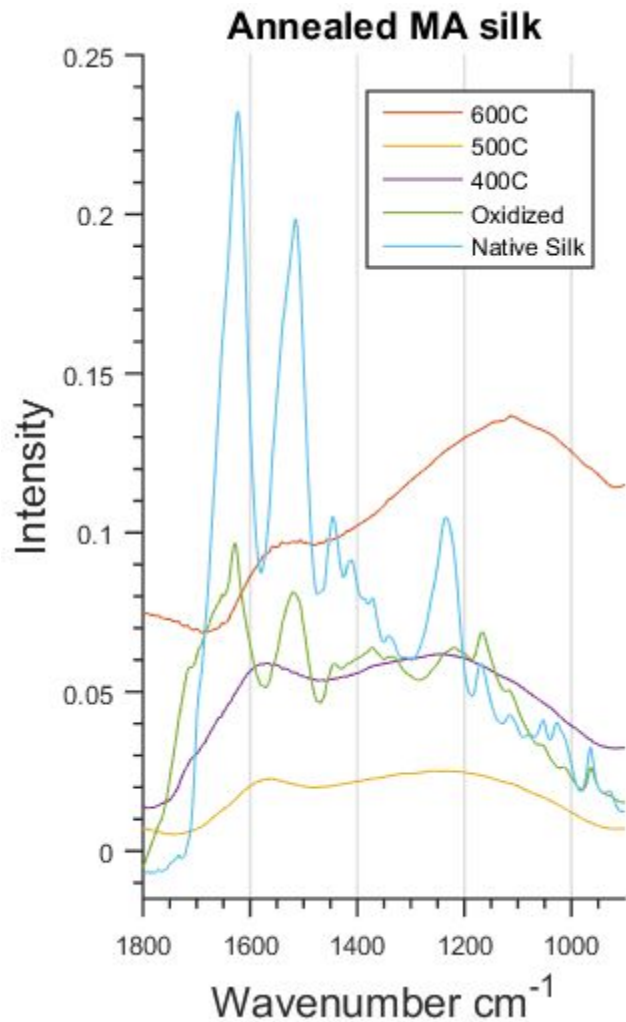


Figure S6. FTIR shows strong amide bands from untreated silk which decrease in intensity upon oxidation and are not present after annealing.

Raman spectra from oxidized fibers were overwhelmed with fluorescence and thus we don't report them. Curve fitting can be a deceptive process, as least-squares fitting algorithms can usually converge a proposed fit, but often using unrealistic values. For consistency, we used 3-peak fits on all Raman spectra unless Origin's algorithm determined the third peak was null. While it is possible additional D bands are present, and fits with less than 3 peaks did converge, these additional peaks did not significantly affect the I_D/I_G values. Initial data from Raman maps of PAN and annealed MA silk suggest significantly more graphite in the silk fiber shell for all

annealing temperatures; however, further investigations are needed to confirm this. The low signal-to-noise ratio in spectra from the shell, likely due to overlap with the embedding resin, makes the spectra sensitive to the type of background subtraction used. This has a pronounced effect on peak fitting and the calculated I_D/I_G . Increasing the

acquisition time or oversampling in the shell region will be helpful, but we leave this for future studies. Additional controls should be run to determine the relative contribution of the spiroin distribution on the core-shell graphitization.

C_λ from the Tuinstra-Koenig relation is calculated by $C_\lambda = C_0 + \lambda_L C_1$, Where $C_0 = 126 \text{ \AA}$ and $C_1 = 0.033$ (data estimated for a sp²-based carbon) and λ_L is the excitation wavelength (1999 Matthews, 1970 Tuinstra, 1998 Knight). For the 473 nm laser used to measure fiber cross-sections, $C_\lambda = 3.0 \text{ nm}$, and $C_\lambda = 5.0 \text{ nm}$. From this, calculating L_α using the Tuinstra-Koenig relationship is straightforward (table S1).

Table S1. I_D/I_G ratios and estimated crystal sizes (nm)

	MA silk		Polyalanine		PAN	
	I_D/I_G	L_α	I_D/I_G	L_α	I_D/I_G	L_α
400 °C	1.21	4.1	0.90	5.5	1.31	3.8
500 °C	1.19	4.2	1.17	4.2	1.33	3.7
600 °C	1.18	4.2	1.15	4.3	1.25	4.0

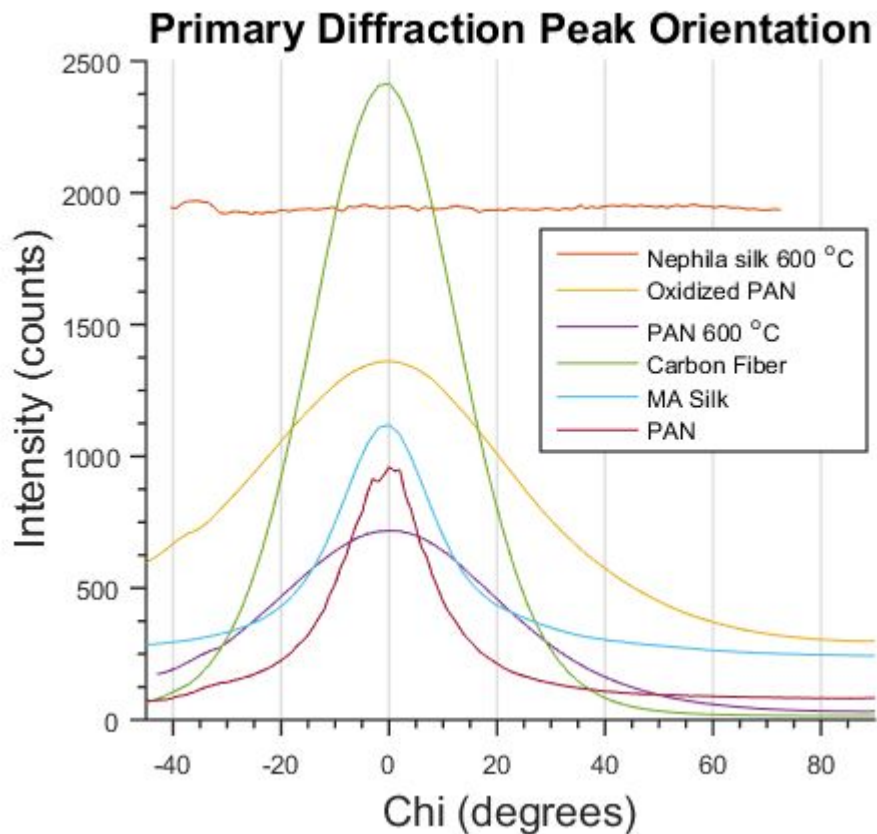


Figure S7. 600 °C annealed fibers, Oxidized PAN, and Carbon fiber plots represent graphite (002). PAN represents the (200). MA silk represents the (020) with some overlap from the (120). Scattering from the beamstop interfered with the orientation calculation from Oxidized silk, so we don't report it.